<u>Appendix:</u>

Appendix table S1: Details for donor retina samples.

Appendix table S2: Breakdown of cell number assigned to individual donor libraries.

Appendix table S3: Membrane-related markers were extracted from GO annotation using the differentially expressed genes in the major human retinal cell types.

Appendix figure S1: Correlation of cell viability of post-mortem human neural retina with post-mortem time and donor age.

Appendix figure S2: Heatmaps of the top 12 principal components explaining the primary sources of heterogeneity in the retinal scRNA-seq data.

Appendix figure S3: Cluster distribution in individual single cell libraries and prediction of cluster relationship between library technical replicates.

Appendix figure S4: Retinal class marker gene expression in unassigned clusters C14 and C5.

Appendix table S1: Details for donor retina samples.

Retina	Patient ID	Eye bulb	Sex	Age (years)	Retrieval time (hrs)	Ocular complications	Assay	scRNA-seq Library	Targeted cell number	Captured cell number after QC
1	17-010	Right	F	80	11.5	Cataract on left eye	scRNAseq, cell viability	A	4000	2122
2	SC	Left	M	42	6.2	-	scRNAseq, cell viability	A	10000	4449
								B	10000	4528
3	17-011	Right	F	53	14.5	-	scRNAseq, cell viability	A	10000	4518
								B	10000	4392
4	16033	Left	M	73	12	-	FISH			
5	16061	Left	M	79	25	-	FISH			
6	16088	Left	F	61	22	-	FISH			
7	16168	Left	M	74	7, 13	-	FISH			
8	17-080	Right	F	77	4.25	-	Cell viability			
9	17-143	Left	M	66	23	-	Cell viability			
10	17-153	Left	M	73	13	-	Cell viability			
11	17-160	Left	F	76	33.75	-	Cell viability			
12	17-167	Right	M	49	16	-	Cell viability			

Appendix table S2: Breakdown of cell number assigned to individual donor libraries. The red highlight the number of cells assigned in the largest clusters, showing similar cell assignment to clusters between 2 replicates.
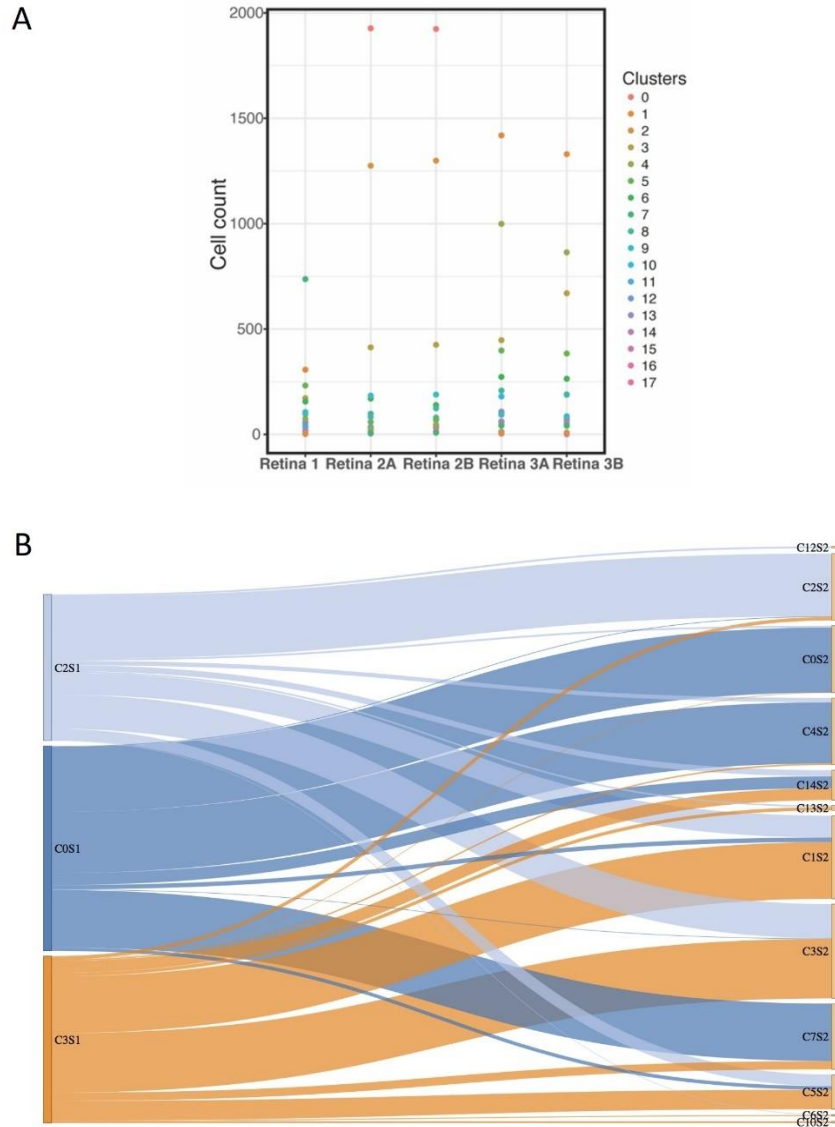
Clusters	Retina 1	Retina 2A	Retina 2B	Retina 3A	Retina 3B
0	58	1927	1924	103	66
1	307	33	30	1419	1330
2	3	1275	1299	9	9
3	172	413	425	447	670
4	74	23	46	999	864
5	232	59	74	398	384
6	156	170	139	273	264
7	737	6	8	42	41
8	97	98	124	208	190
9	106	184	189	93	86
10	33	83	80	180	188
11	42	83	68	93	77
12	55	35	35	108	82
13	18	20	40	58	51
14	14	7	11	62	71
15	11	4	12	13	9
16	5	8	11	9	9
17	2	21	13	4	1

Appendix table S3: Membrane-related markers were extracted from GO annotation using the differentially expressed genes in the major human retinal cell types. * Genes potentially involved in membrane interaction or membrane trafficking.

Cell types	Identified membrane-related markers
Rod photoreceptors	*RHO, ROM1, CNGA1, CNGB1, PRPH2, MFGE8*
Cone photoreceptors	*OPN1LW, SLC24A2, DST, TTR**
Muller glia	*RGR, GPR37, RLBP1*, NCAM1, CD164*
Horizontal cells	*CNTNAP2, PTN, NDRG4*, TAGLN3*
Bipolar cells	*TRPM1, GRM6*
Amacrine cells	*EPHB6, SLC5A7, GABRD, KCNJ12, PTPRF, GRIN2A*
Retinal astrocytes	*GYPC, SERPINA5, CD44, SLC4A4, AQP4, ABCC3, NGFR*
Microglia	*CD74, HLA-DRA, HLA-DPA1, TYROBP*, FCER1G, LAPTMS, CD14, HLA-DQA1, FXYD5, CTSB*, CD37*
Retinal ganglion cells	*RTN1*, NDRG4*, UCHL1*, YWHAH**
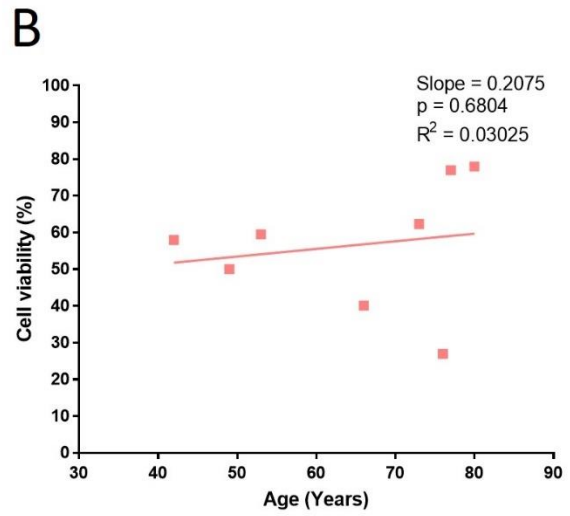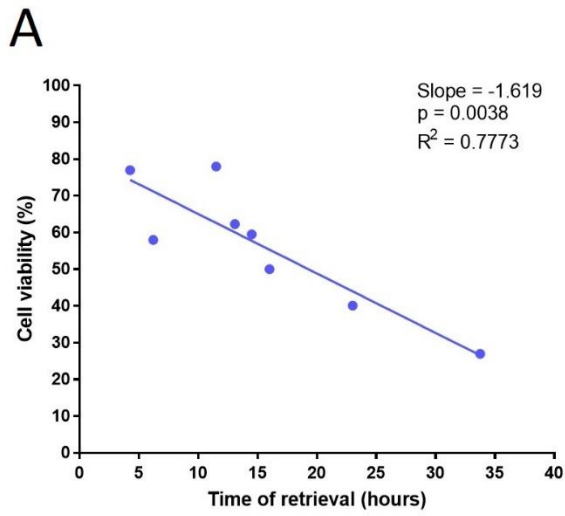
Appendix figure S1: Correlation of cell viability of post-mortem human neural retina with A) time of tissue retrieval after death, and B) age of donor.

Appendix figure S2: Heatmaps of the top 12 principal components explaining the primary sources of heterogeneity in the retinal scRNA-seq data. Cells and genes are ordered by PCA score calculated by Seurat. The genes driving the majority of the variance are determined using the top 500 cells.

Appendix figure S3: A) Distribution of frequency of the 18 clusters in individual single cell libraries showing donor-specific clusters corresponding to rod photoreceptors (C0, C1, C4). B) Prediction of cluster relationship between library technical replicates in Retina 1 and Retina 2. The Sankey plot shows edges connecting clusters, with larger edge indicating higher similarity, ranging from 0 to 100%. The size of the edge was quantitatively estimated by implementing scGPS modelling approach for pairs of clusters, as described in the method section. The three largest clusters in Retina 2A were compared with all clusters in Retina 2B. Consistently we see C2 in Retina 2A is most similar to C2 in Retina 2B. The same trend is seen for C0 and C3. These results demonstrated that the variation between library replicates is minimal in our dataset, and that the clusters determined from the merged dataset were consistent across samples. We also found higher similarities among Rod photoreceptor clusters (C0, 2, 3 in Retina 2A with clusters C0, 2, 4, 7 in Retina 2B) than compared with other clusters.
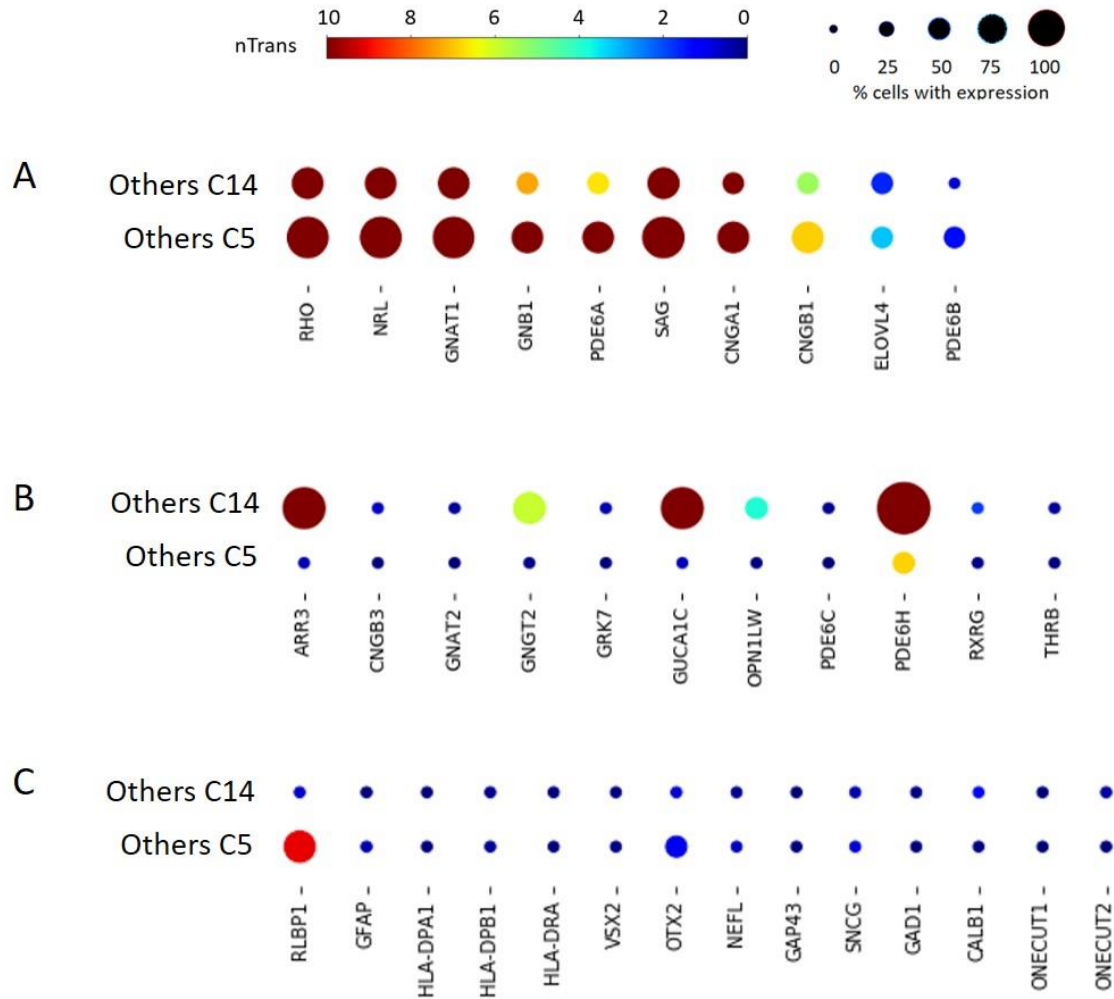
Appendix figure S4: Feature expression heatmap showing expression patterns of A) rod photoreceptor markers, B) cone photoreceptor markers and C) other major retinal class markers (Müller glia: RLBP1; astrocytes: GFAP; microglia: HLA-DPA1, HLA-DPB1, HLA-DRA; Bipolar cells: VSX2, OTX2; retinal ganglion cells: NEFL, GAP43, SNCG; Amacrine cells: GAD1, CALB1; Horizontal cells: ONECUT1, ONECUT2) in unassigned clusters C14 and C5. The size of each circle depicts the percentage of cells expressing the marker within the cluster.